

# Influence of topology of LCST-based graft copolymers on responsive assembling in aqueous media



Hui Guo <sup>a, b</sup>, Annie Brûlet <sup>c</sup>, Pattuparambil R. Rajamohanan <sup>d</sup>, Alba Marcellan <sup>a, b</sup>,  
Nicolas Sanson <sup>a, b</sup>, Dominique Hourdet <sup>a, b, \*</sup>

<sup>a</sup> École Supérieure de Physique et de Chimie Industrielles de la Ville de Paris (ESPCI), ParisTech, PSL Research University, Sciences et Ingénierie de la Matière Molle, CNRS UMR 7615, 10 rue Vauquelin, F-75231 Paris Cedex 05, France

<sup>b</sup> Sorbonne-Universités, UPMC Univ Paris 06, SIMM, 10 rue Vauquelin, F-75231 Paris Cedex 05, France

<sup>c</sup> Laboratoire Léon Brillouin (CNRS UMR 12), CEA Saclay, F-91191 Gif-sur-Yvette Cedex, France

<sup>d</sup> Central NMR Facility, CSIR-National Chemical Laboratory, Pune 411 008, India

## ARTICLE INFO

### Article history:

Received 21 November 2014

Received in revised form

14 January 2015

Accepted 16 January 2015

Available online 24 January 2015

### Keywords:

Poly(*N*-isopropylacrylamide)

Thermothickening

Associating polymers

## ABSTRACT

This work, based on structure/properties relationships of associating polymers, aims to investigate the role of topology in the self-assembling behavior of responsive graft copolymers. For that purpose, two graft copolymers with inverse topologies were prepared with similar amounts of water-soluble chains (poly(*N,N*-dimethylacrylamide) = PDMA) and LCST polymer chains (poly(*N*-isopropylacrylamide) = PNIPA). In pure water, and above 3 wt%, PNIPA-*g*-PDMA and PDMA-*g*-PNIPA exhibit very similar macroscopic properties with a sol/gel transition above 35 °C related to the micro-phase separation of PNIPA sequences. From complementary experiments, performed by DSC, <sup>1</sup>H NMR and small angle neutron scattering, we show that the phase transition of PNIPA is more abrupt when NIPA units are located within the backbone, compared to side-chains. Nevertheless, well above their transition temperature, the two copolymers display very similar bicontinuous structures where PNIPA sequences self aggregate into concentrated percolating domains (about 70 wt% at 60 °C) characterized by a frozen dynamics. On the other hand, when salt or surfactant molecules are added into unentangled semi-dilute aqueous solution, the PNIPA-*g*-PDMA sample does not percolate anymore above the transition temperature while PDMA-*g*-PNIPA still demonstrate thermothickening properties that are correlated to the ability of water-soluble PDMA chains to bridge PNIPA aggregates.

© 2015 Elsevier Ltd. All rights reserved.

## 1. Introduction

Associating polymers have known a tremendous development during the last decades due to their enhanced viscoelastic properties that find applications in a wide range of domains like food, cosmetics, paints, drilling fluids, etc [1–3]. In this framework, responsive polymers, that are able to change their macroscopic behavior under environmental conditions like ionic strength, pH, temperature, light, red-ox activity or under external fields (electric or magnetic), are

very useful for applications where enhanced properties are needed under certain conditions [4–6]. Among these various mechanisms, temperature is a common trigger that naturally occurs in many applications and thermoresponsive polymers have known a large development in different fields like oil recovery or biomedical applications [7–12]. Indeed, these systems can be efficiently used to increase or to control the viscosity of drilling fluids submitted to large temperature gradients in deep formations or to promote sol/gel transitions around body temperature with applications like injectable hydrogels and controlled drug release [3,12,13].

Although cellulosic derivatives [14,15] were the first thermothickeners to be used in aqueous media, thermoresponsive systems have been widely diversified during the last two decades [4,7,16]. They are generally designed on the basis of block or graft architectures containing hydrophilic and water-soluble moieties alternating with responsive blocks or grafts characterized by a Lower Critical Solution Temperature (LCST) in the range of application.

\* Corresponding author. Sorbonne-Universités, UPMC Univ Paris 06, SIMM, 10 rue Vauquelin, F-75231 Paris Cedex 05, France. Tel.: +33 (0)1 40 79 46 43; fax: +33 (0)1 40 79 46 86.

E-mail addresses: [hui.guo@espci.fr](mailto:hui.guo@espci.fr) (H. Guo), [brulet@llb.saclay.cea.fr](mailto:brulet@llb.saclay.cea.fr) (A. Brûlet), [pr.rajamohanan@ncl.res.in](mailto:pr.rajamohanan@ncl.res.in) (P.R. Rajamohanan), [alba.marcellan@espci.fr](mailto:alba.marcellan@espci.fr) (A. Marcellan), [nicolas.sanson@espci.fr](mailto:nicolas.sanson@espci.fr) (N. Sanson), [dominique.hourdet@espci.fr](mailto:dominique.hourdet@espci.fr) (D. Hourdet).

Quite a lot of systems, mainly based on poly(*N*-alkylacrylamide) and poly(alkylene oxide) have been reported with various level of understanding of their structure/properties relationships [17–23]. For these copolymers the key parameters are the chemical nature of both LCST and hydrophilic sequences as well as the design of associating copolymers (distribution and relative ratio between hydrophilic and “hydrophobic” moieties) that directly impact the level of the phase segregation (from nano to macroscopic scale) and the final properties of aqueous formulations.

In the case of thermothickening copolymer solutions, designed with poly(ethylene oxide-co-propylene oxide) derivatives, the LCST sequences self-assemble into liquid-like aggregates above their transition temperature. These hydrophobic domains behave as efficient physical cross-links and viscoelastic analysis highlight the dynamic properties of these systems with a finite lifetime of the responsive stickers [16,22]. By comparison poly(*N*-isopropylacrylamide) (PNIPA) behaves rather differently as during the phase transition the PNIPA-rich phase reaches the so-called Berghmans point where it is supposed to become glassy [24,25]. Although this assumption remains controversial [26], the formation of frozen PNIPA domains above their transition temperature is often taken into account to explain the formation of stable colloidal PNIPA particles at high temperature with ineffectiveness of colloid aggregation [27] or the extraordinarily slow deswelling of macroscopic PNIPA hydrogels; the out-of equilibrium state of the gel being conserved for many days [28].

In the framework of thermothickeners with grafted architectures, the phase transition driven by LCST moieties must remain confined at a local scale to avoid the macro-phase separation and the ruin of the elastic properties. Although most of thermoresponsive graft copolymers are generally designed with a hydrophilic backbone and LCST side-chains [7,16], the inverse topology is also conceivable with similarities with weakly ionized PNIPA chains where electrostatic repulsions stabilized the transient network formed at high temperature [29]. Amazingly, if we except some theoretical works [30,31,32], a direct comparison between 3D self-assemblies of graft copolymers with similar composition but inverse topology (see Fig. 1) has never been investigated so far although this comparison naturally raises a lot of questions about the structure/properties relationships. For instance we can reasonably wonder how these graft copolymers with inverse topologies will behave below and above the transition temperature? How the responsivity of LCST stickers (association temperature, concentration of polymer rich phase...) will be affected by the topology? What will be the microstructure of 3D self-assemblies and the corresponding viscoelastic properties? What will be the relative sensitivity of these copolymers to environmental modifications induced by adding cosolute?

In order to address the topological issue in thermoassociating graft copolymers, grafted macromolecules were prepared with similar amounts of water-soluble chains (poly(*N,N*-dimethylacrylamide) = PDMA) and LCST polymer chains (poly(*N*-isopropylacrylamide) = PNIPA) which exhibit a LCST around 32 °C in water. These two *Yin and Yang* copolymers (PNIPA-g-PDMA and PDMA-g-PNIPA), sharing identical monomers with inverse topology, are represented in Fig. 1.



Fig. 1. Schematic representation of *Yin and Yang* graft copolymers prepared from PDMA (—) and PNIPA (—).

Based on this set of copolymers, a detailed comparative study has been performed on semi-dilute solution as a function of temperature and added molecules like salt or surfactant. This original analysis, carried out by rheology, differential scanning calorimetry, NMR and light/neutron scattering techniques, surprisingly highlights very common features as well as large differences between the two copolymers that could be understood from their topology.

## 2. Experimental section

### 2.1. Materials

*N*-isopropylacrylamide (NIPA, Aldrich), *N,N*-dimethylacrylamide (DMA, Aldrich), cysteamine hydrochloride (AET·HCl, Fluka), potassium peroxydisulfate (KPS, Aldrich), acrylic acid (AA, anhydrous > 99%, Fluka), dicyclohexylcarbodiimide (DCCI, Aldrich), ammonium persulfate (APS, Aldrich), sodium metabisulfite (SBS, Aldrich) were used as received. All organic solvents were analytical grade and water was purified with a Millipore system combining inverse osmosis membrane (Milli RO) and ion exchange resins (Milli Q) for synthesis and purification.

### 2.2. Synthesis of thermosensitive linear copolymers

The synthesis of responsive linear copolymers was performed according to a three-step process. Telomers were first synthesized through free radical polymerization. Then, the macromonomers were obtained by coupling amino-terminated telomers with acrylic acid and finally graft copolymers were prepared by free radical polymerization of monomers and macromonomers. An example is given in Fig. 2 in the case of PDMA-g-PNIPA and the detailed procedure is described in Supporting Information. In order to simplify the nomenclature of the copolymers, PNIPA-g-PDMA and PDMA-g-PNIPA will be named PN-D and PD-N, respectively.

### 2.3. Size exclusion chromatography (SEC)

Experiments were carried out with two different chromatographic systems. The first one, which was applied to the absolute characterization of polymer samples, is a Viscotek triple detector (TDA 302) equipped with three columns (OH-pak). During the analysis carried out at 28 °C the flow rate was controlled at 0.6 mL min<sup>-1</sup> using 0.2 M NaNO<sub>3</sub> as mobile phase. The molar masses were derived from a universal calibration curve based on Pullulan standards from Sopares (OmniSEC software). The other chromatographic system from Waters is equipped with similar Shodex OH-pak columns thermostated at 10 °C and a differential refractometer (Shimadzu RID-10A). This system was mainly used to follow, without purification, the conversion of the reactions. The flow rate was controlled at 0.90 mL min<sup>-1</sup> using 0.5 M LiNO<sub>3</sub> as mobile phase.

### 2.4. Nuclear magnetic resonance (NMR)

All the NMR measurements were performed on a Bruker Avance III HD spectrometer operating at 700 MHz for <sup>1</sup>H, using a standard

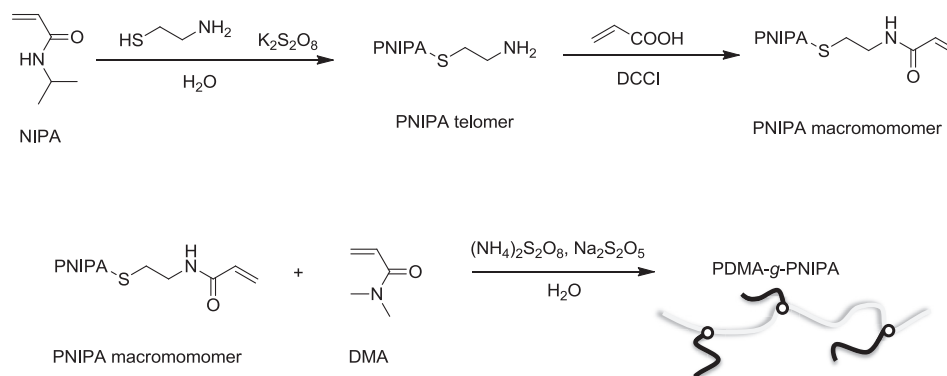


Fig. 2. Three-step synthesis of graft copolymers exemplified with PDMA-g-PNIPA (PD-N).

5 mm broadband Smart probe. The temperature control was achieved by a Bruker BCU II unit and a build in temperature control unit. Following experimental conditions were employed for the variable temperature experiments: 32 transients, 45° flip angle, 2.5 s acquisition time, 2 s relaxation delay. The sample was allowed to equilibrate for ~10 min at each temperature. The  $^1\text{H}$  chemical shifts were referred to residual HOD peak at each temperature [33]. 3 wt % solutions of PD-N and PN-D in  $\text{D}_2\text{O}$  were used for the NMR measurements.

### 2.5. Rheology

The viscoelastic properties of the copolymers were studied in aqueous solutions, in the semi-dilute regime, using a stress-controlled rheometer (AR 1000 from TA Instruments) equipped with a cone/plate geometry (diameter 40 mm, angle 2, truncature 55.9  $\mu\text{m}$ ). The experiments were performed in the linear viscoelastic regime which was established for each sample by a stress sweep at the lowest frequency. The temperature was controlled by a high power Peltier system that provides fast and precise adjustment of the temperature during heating and cooling stages. Typically, the experimental conditions were fixed at constant frequency (1 Hz) and shear stress (2 Pa). A particular care was taken to avoid the drying of the sample by using a homemade cover which prevents from water evaporation during experiment. In these conditions, dynamic moduli ( $G'$  and  $G''$ ) as well as complex viscosity ( $\eta^*$ ) were recorded between 20 and 60 °C by applying heating and cooling scans of 2 °C  $\text{min}^{-1}$ .

### 2.6. Differential scanning calorimetry (DSC)

The phase transition of PNIPA-based copolymers in aqueous solution was investigated by Differential Scanning Calorimetry using a DSC Q200 from TA instrument. Polymer solutions (80 mg), equilibrated with a reference filled with the same quantity of solvent, were submitted to temperature cycles between 10 and 70 °C. The heating and cooling rates were similarly fixed at 2 °C  $\text{min}^{-1}$ .

### 2.7. Dynamic light scattering (DLS)

Dynamic Light Scattering (DLS) was carried out on a CGS-3 goniometer system equipped with He–Ne laser illumination at 633 nm and an ALV/LSE-5003 correlator. All samples were initially filtered through 0.45  $\mu\text{m}$  Millipore syringe filters. The samples were stabilized at constant temperature for 10 min prior to measurement. The data were collected by monitoring the light intensity at a scattering angle of 90°. DLS experiments were performed on dilute solution (0.1  $\text{g L}^{-1}$ ) and each measurement lasts 120 s.

### 2.8. Small angle neutron scattering (SANS)

SANS experiments were performed at Laboratoire Léon Brillouin (CEA-Saclay, France) on the PAXY spectrometer. The wavelength of the incident neutron beam was set at  $\lambda = 12 \text{ \AA}$  with a corresponding sample-to-detector distance of 4.7 m. This configuration provides a scattering vector modulus [ $q = 4\pi/\lambda \sin(\theta/2)$ ] ranging between 0.002 and 0.04  $\text{\AA}^{-1}$  (where  $\theta$  is the scattering angle). All the samples were prepared at room temperature in  $\text{D}_2\text{O}$  and transferred into 2- or 5-mm-thick quartz containers for SANS experiments. For the data treatment, the scattering from the empty quartz cell was subtracted, the efficiency of the detector cell was normalized by the intensity delivered by a pure water cell of 1-mm thickness and absolute measurements of the scattering intensity  $I(q)$  ( $\text{cm}^{-1}$  or  $10^{-8} \text{ \AA}^{-1}$ ) were obtained from the direct determination of the incident neutron flux and the cell solid angle.

## 3. Results

### 3.1. Synthesis and characterization of graft copolymers

Let us first recall that PN-D has PNIPA backbone and graft PDMA chains, while PD-N has the inverse topology with PDMA backbone and PNIPA grafts. Graft precursors and copolymers were characterized by  $^1\text{H}$  NMR and SEC (Table 1). In the case of amino-terminated PDMA and PNIPA, the molar masses are 15 and 23  $\text{kg mol}^{-1}$ .

Table 1  
Structural characterization of linear copolymers.

Copolymers	Molar mass and dispersity index		Molar (weight) monomer ratio in backbone/grafts from feed monomer composition	Molar (weight) monomer ratio in backbone/grafts from copolymer composition
	Graft	Graft copolymer		
PD-N	$M_n = 23.0 \text{ kg/mol}$ $\mathcal{D} \cong 1.4$	$M_n = 370 \text{ kg/mol}$ $\mathcal{D} \cong 2.6$	1.14/1 (50/50)	1.44/1 (56/44)
PN-D	$M_n = 14.5 \text{ kg/mol}$ $\mathcal{D} \cong 1.5$	$M_n = 460 \text{ kg/mol}$ $\mathcal{D} \cong 2.7$	1/1.14 (50/50)	1.12/1 (56/44)

mol, respectively, in good agreement with similar telomerizations performed with NIPA, DMA and other hydrophilic comonomers [34,35].

After coupling the amino end-group with a large excess of acrylic acid, and assuming a quantitative yield of this reaction, we can see that the level of macromonomer incorporation in the graft copolymer is relatively high for the two macromonomers.  $^1\text{H}$  NMR analysis gives a relative conversion of about 80% for the copolymerization of vinyl-terminated PDMA and PNIPA with respect to the other comonomer. Starting from the same feed **monomer/(macromonomer)** weight ratio (**50/(50)**), the final weight composition of graft architectures is **56/(44)** for both PN-D and PD-N. Even if these topologically inverse copolymers do not have exactly the same DMA/NIPA weight content, their equilibrated composition remains in good agreement with our initial goal as it provides a good compromise between solubility and aggregation at high temperature. Moreover, the high molar mass of the copolymer chains ( $M_n \sim 400$  kg/mol) is favorable for the physical gel formation, as high molar mass means 1) low overlap concentration with the possibility to develop a percolated network at low concentration, and 2) a higher number of side-chains per macromolecule (between 8 and 12 in average for PD-N and PN-D) increasing the probability of inter-chain contacts.

### 3.2. Thermothickening behavior: sol/gel transition

As shown in Fig. 3, the two copolymer solutions studied at 3 wt% in the linear regime exhibit very similar thermothickening properties.

At low temperature, typically below 35 °C, the backbone and the side chains are soluble in water and the copolymer solutions are mainly fluids with a very weak elastic contribution that is negligible and not measurable in our conditions. In this range of temperature the complex viscosity (see Fig. S1 in Supporting Information), which is also the Newtonian viscosity at this frequency, decreases smoothly following an Arrhenius dependence. When the transition takes place, above  $T_{as} = 35$  °C, PNIPA sequences start to self-associate giving rise to a sol/gel transition with a huge increase of elasticity, mainly between 35 and 45 °C. Then at high temperature, ( $T > 45$ –50 °C), well above the phase transition, the dynamic moduli and particularly the elastic one still increases slightly with temperature. In these conditions, the copolymer solutions behave as elastic gels with a very weak frequency dependence of the modulus and very long relaxation times which are out of scale in

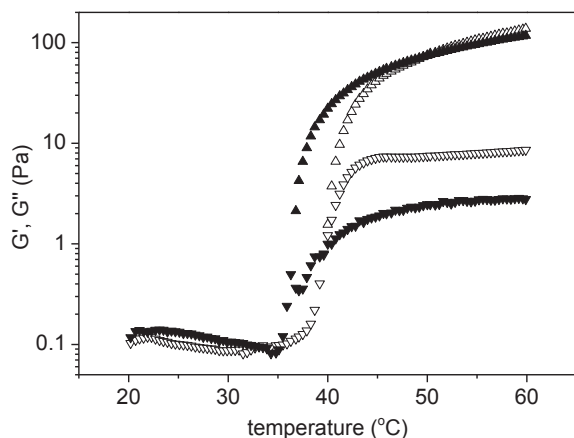


**Fig. 3.** Temperature dependence of dynamic moduli ( $\blacktriangle$ ,  $\triangle$  for  $G'$  and  $\nabla$ ,  $\triangledown$  for  $G''$ ) of PD-N (hollow symbols) and PN-D (filled symbols) aqueous solutions ( $C_p = 3$  wt %,  $f = 1$  Hz, heating rate = 2 °C  $\text{min}^{-1}$ ).

these experiments (see Fig. S2 in Supporting Information). Here, we have to mention that the associating process is totally reversible with temperature with almost no hysteresis in the conditions of the study (see Fig. S1). Interestingly, the two graft copolymers display very similar thermothickening properties that emphasize at the first order a common self-assembling process despite their inverse topologies. The main difference that can be underlined from Fig. 3 is the rise of the elastic modulus that takes place a few degrees before for PN-D solution compared to PD-N. From another macroscopic point of view, the two copolymer solutions, initially transparent, remain translucent above the association temperature but more whitish for PN-D. By comparison, graft copolymers prepared by grafting shorter PNIPA side chains onto well water-soluble backbones like poly(sodium acrylate) or polyacrylamide remain totally transparent, even at high temperature and for high fraction of responsive stickers [23,34,35].

### 3.3. Phase transition

The LCST-type phase transition of PNIPA in aqueous solutions is a very well-known phenomenon that has been widely reported in the literature [24,36]. At low temperature, PNIPA chains are soluble in water and exhibit a coiled conformation in order to maximize their hydrogen bonds with water molecules. Crossing the transition temperature, the chains start to undergo a sharp coil-to-globule transition in water, changing from hydrophilic state to hydrophobic one. During demixing, energy is required to disrupt the interactions between water molecules and amide groups and the phase transition of PNIPA is an endothermic process that can be easily followed by calorimetry. For instance, DSC experiments have shown that the characteristic parameters of the transition, typically the temperature and the transition enthalpy, are strongly coupled to the structure of the chain (molar mass, chemical composition and topology) and to the environmental conditions (pH, ionic strength, co-solvent ...) [24,36–38]. A typical thermogram is given in inset of Fig. 4 for a 3 wt% aqueous solution of PN-D, along with the transition enthalpies ( $\Delta H$  in kJ/mol of NIPA) of PN-D and PD-N solutions obtained after integration of endotherms.

The two copolymer solutions are characterized by a rather broad endotherm that spans over 10 °C as already observed for the viscoelastic transition in Fig. 3. The broadness of the transition does not originate from the relatively high heating rate applied in DSC

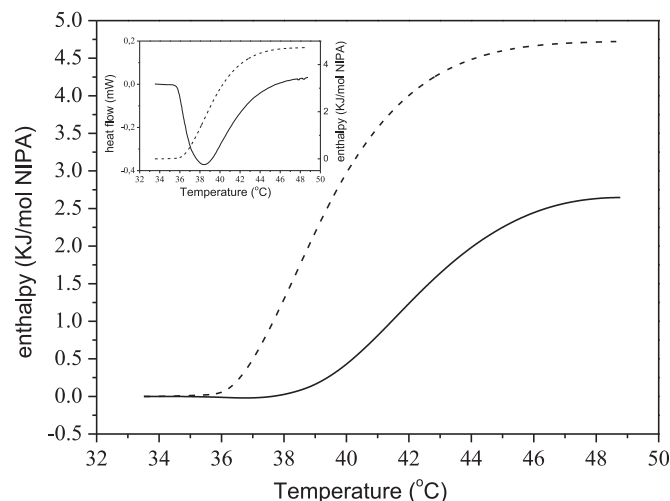


**Fig. 4.** DSC analysis of PN-D (dash line) and PD-N (solid line) aqueous solution ( $C_p = 3$  wt %, heating rate = 2 °C  $\text{min}^{-1}$ ). The thermogram of PN-D (heat flow vs temperature) and its integration (cumulated enthalpy) are shown in inset.

( $2\text{ }^{\circ}\text{C min}^{-1}$ ), since similar thermograms were obtained at lower rates. For instance,  $T_{as}$  and transition width decrease of approximately  $1\text{ }^{\circ}\text{C}$  by decreasing the heating rate from  $2$  to  $0.5\text{ }^{\circ}\text{C min}^{-1}$  while the transition enthalpy remains unchanged. The transition broadness probably arises from the relatively low molar mass of PNIPA sequences and their dispersity index but the topology of PD-N and PN-D, alternating PNIPA with hydrophilic PDMA inside the same covalent structure, certainly accounts for this behavior. As we can see from Fig. 4, similar endotherms were obtained for both copolymers upon increasing temperature but the PN-D sample with the PNIPA backbone definitely shows the highest enthalpy ( $4.7\text{ kJ/mol NIPA}$ ) and the lowest transition temperature ( $36\text{ }^{\circ}\text{C}$ ). By comparison, the transition of the PD-N solution starts at slightly higher temperature ( $\sim +2\text{ }^{\circ}\text{C}$ ), around  $38\text{ }^{\circ}\text{C}$ , with an enthalpy of  $2.6\text{ kJ/mol NIPA}$ : the architecture of PD-N with PNIPA as pendant chains does not favor the association process between grafted chains that are not topologically close to each other. By comparison, the PNIPA precursor of the PD-N copolymer displays a lower association temperature ( $T_{as} = 36\text{ }^{\circ}\text{C}$ ) and a higher transition enthalpy ( $\Delta H = 4.3\text{ kJ/mol NIPA}$ ) at the same relative concentration. This comparison supports the idea that there is some energetic barrier in the association process due to the steric hindrance from the water-soluble backbone.

Complementary experiments have been carried out by  $^1\text{H NMR}$  as a function of temperature. From the series of NMR spectra obtained between  $15$  and  $55\text{ }^{\circ}\text{C}$  with the PD-N solution (Fig. 5a), we can see that the signal of methyl groups of DMA, around  $3\text{ ppm}$ , becomes to broaden with increasing temperature but its area remains almost unchanged or just slightly decreases with increasing temperature as reported in Fig. 5b.

In the same conditions, the signals of methyl and methine groups of NIPA, observed at  $1$  and  $4\text{ ppm}$  respectively, show a dramatic decrease above  $35\text{ }^{\circ}\text{C}$  and practically disappear at  $55\text{ }^{\circ}\text{C}$ . This feature, that has been widely reported with PNIPA copolymers or gels [39–42], can be assigned to the formation of a solid-like rich-PNIPA phase close to its glass transition [24] and where the motions of the functional groups are strongly reduced. As shown in Fig. 5b, the PN-D sample undergoes a more abrupt transition than PD-N as already described by DSC. The main conclusion that holds for the two copolymer solutions, is that at high temperature most of PNIPA sequences are aggregated into PNIPA-rich domains of low mobility. The low exchange rate of PNIPA sequences at high temperature is also responsible for the “covalent network” pattern

obtained with the two copolymers in the gel state (Fig. S2 in Supporting Information).

#### 3.4. Nanostructure from small angle neutron scattering

Scattering experiments have been performed at different temperatures with copolymer solutions in  $\text{D}_2\text{O}$ . As shown in supporting information (Fig. S3), there is no significant modification of the thermodynamic behavior of PNIPA replacing  $\text{H}_2\text{O}$  with  $\text{D}_2\text{O}$ ; or at least the difference remains within  $1\text{ }^{\circ}\text{C}$  as already reported in the literature [43]. As shown in Fig. 6a, the thermo-association process of PN-D in aqueous solution takes place abruptly upon heating. As soon as the transition temperature is reached, above  $33\text{ }^{\circ}\text{C}$  as measured in the sample holder, the scattering intensity immediately increases on the whole  $q$ -range figuring fluctuation concentrations related to the phase separation of PNIPA. With increasing temperature, the intensity still increases with a characteristic length that can be more easily observed at higher polymer concentrations (see Fig. 7a). This means that hydrophilic PDMA side-chains efficiently stabilize the phase separation process of PNIPA backbone at a microscopic level; the characteristic size of the micro-phase separation being  $D = 2\pi/q_{max}$ . Concurrently, as soon as the transition takes place, the Porod's law ( $I(q) \sim q^{-4}$ ) is observed in the asymptotic regime, in agreement with the formation of a biphasic system with sharp interfaces.

By comparison, the thermo-association process of PD-N in aqueous solution takes place more progressively upon heating. As soon as the transition temperature is reached, the scattering intensity starts to increase at low  $q$  with the formation of heterogeneities at long distance. Then, above  $35\text{ }^{\circ}\text{C}$ , the scattering intensity increases progressively and its  $q$ -dependence finally reaches the Porod's law at high temperature, above  $45\text{--}50\text{ }^{\circ}\text{C}$ . These scattering patterns, typical from microphase separation, have been already described for water-soluble polymers grafted with PNIPA or other LCST side-chains [18,44] and for weakly charged PNIPA gels [45] or linear copolymers [29]. From Fig. 7, we notice that at high temperature the two microphase separated systems are characterized by similar correlation lengths, about  $500\text{ \AA}$ . Nevertheless, the PN-D solution clearly shows a higher upturn at low  $q$  (higher osmotic compressibility) underlining the presence of concentration fluctuations at closer distance. This can be related to a decrease of the contribution of PDMA side-chains to steric repulsions with increasing temperatures.

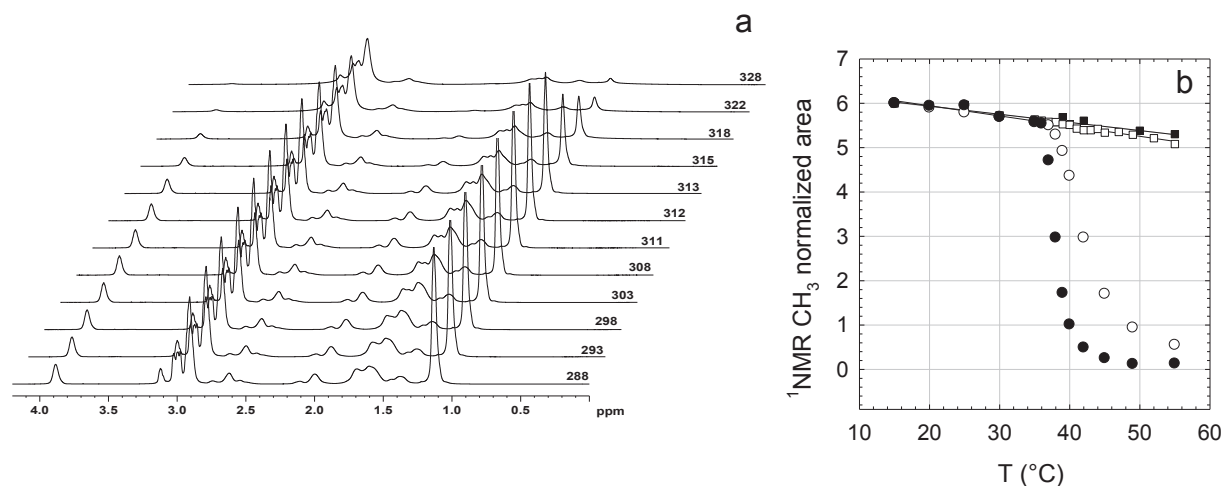
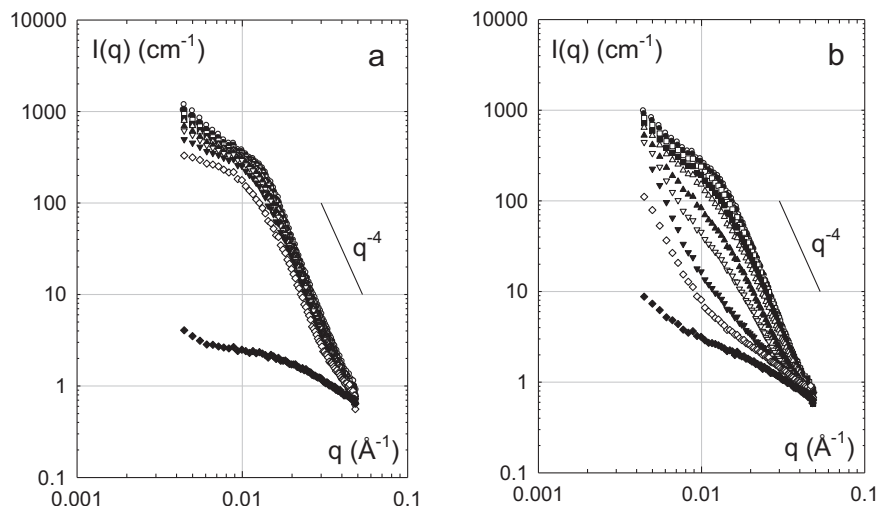


Fig. 5. (a) Temperature variation of  $^1\text{H NMR}$  spectrum of PD-N and (b) normalized area of  $\text{CH}_3$  signal from DMA (square) and NIPA (circle) of PD-N (hollow symbols) and PN-D (filled symbols) aqueous solutions ( $C_p = 3\text{ wt\%}$ ,  $\text{D}_2\text{O}$ ).



**Fig. 6.** Double logarithmic plots of the scattering intensity of 3 wt% PN-D (a) and PD-N (b) solutions at different temperatures ( $T$  °C): 33.0 (◆), 35.0 (◇), 36.0 (▼), 37.0 (▽), 38.5 (▲), 40.0 (△), 43.0 (■), 45.5 (□), 51.0 (●) and 57.5 (○).

In order to get more details on the formation of PNIPA domains, the experimental invariant ( $Q_{exp}$ ) was determined from the scattering curve:

$$Q_{exp} = \int_0^{\infty} q^2 I(q) dq \quad (1)$$

In the case of incompressible biphasic systems, as it is for PNIPA copolymer solutions above their transition temperature, the invariant is in theory a constant that only depends on volume fraction ( $\phi_i$ ) and difference between the scattering length densities (the contrast ( $\rho_i$ )) of the two phases:

$$Q_{th} = 2\pi^2 (\rho_1 - \rho_2)^2 \phi_1 \phi_2 \quad (2)$$

As the contrast  $(\rho_1 - \rho_2)^2$  itself is a function of the scattering length density and volume fraction of the phase component, it is then possible to estimate the composition of the segregated phase. Here we assume that PDMA segments are totally excluded from the

segregated phase and remain in the outer medium with water and possibly a fraction of non aggregated PNIPA chains ( $1 - f_{PNIPA}$ ). On this basis, two extreme hypotheses can be considered:

- 1) all PNIPA segments are embedded into micro-domains ( $f_{PNIPA} = 1$ ) at a volume fraction  $\phi_{PNIPA} < 1$ ; considering the presence of water inside the aggregates,
- 2) only a fraction of PNIPA chains ( $f_{PNIPA} < 1$ ) contributes to the formation of dry aggregates ( $\phi_{PNIPA} = 1$ ).

As shown in supporting information (Fig. S4), the extrapolated values of  $f_{PNIPA}$  times  $\phi_{PNIPA}$  do not strongly differ from one hypothesis to the other. Considering that all the other situations lie between these two limits, we have used the average value of  $f_{PNIPA} \cdot \phi_{PNIPA}$  in the following discussion to describe the “level of the phase separation”. Such data treatment is exemplified in Fig. 8 with PN-D and PD-N solutions at 3 and 8 wt% in water. As we can see, the self-assembling of PNIPA sequences mainly takes place between 35 and 45 °C where the level of the phase separation reaches about

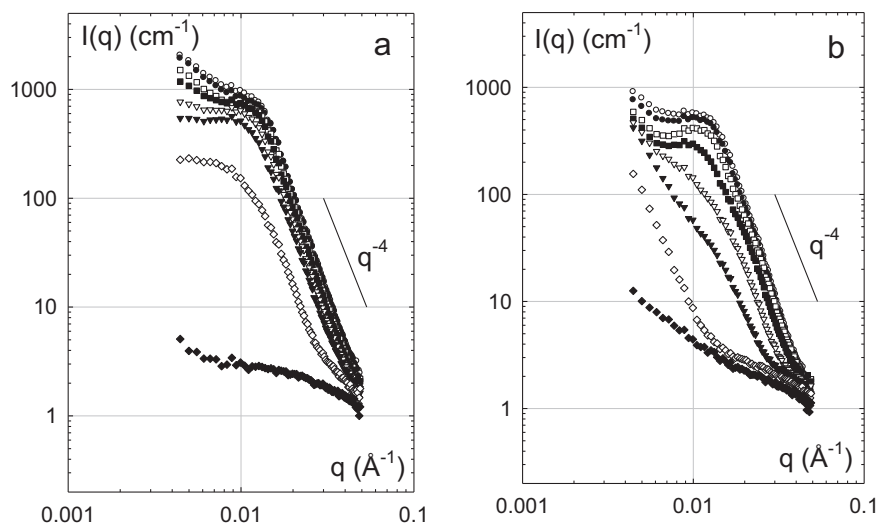


**Fig. 7.** Double logarithmic plots of the scattering intensity of 8 wt% PN-D (a) and PD-N (b) solutions at different temperatures ( $T$  °C): 29.0 (◆), 33.0 (◇), 35.0 (▼), 36.0 (▽), 38.5 (■), 43.0 (□), 51.0 (●) and 57.5 (○).

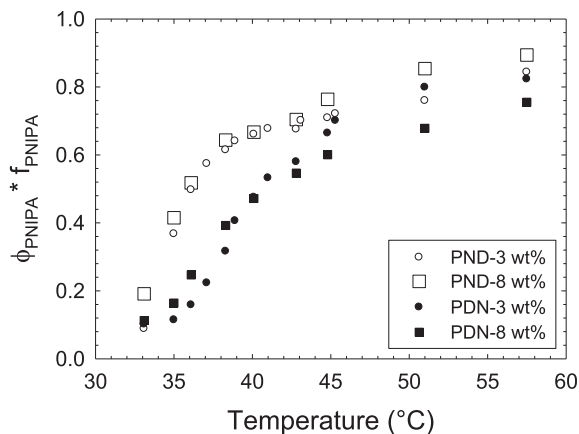


Fig. 8. Temperature dependence of the PNIPA-rich phase with  $f_{\text{PNIPA}}$  the fraction of PNIPA embedded in the segregated phase and  $\phi_{\text{PNIPA}}$  their volume fraction estimated from the SANS invariant analysis.

60–70%, with a relative accuracy of about 10%. Above 45 °C, the extent of the phase segregation increases more gently up to 70–80% at 60 °C. These results are in good agreement with previous data obtained by DSC,  $^1\text{H}$  NMR and rheology where the PD-N sample (with PNIPA grafts) was shown to self-associate more gradually with temperature compared to the inverse PN-D structure (with PNIPA backbone). Above 45 °C, the phase transition is almost over for PN-D, as seen from DSC and NMR ( $f_{\text{PNIPA}} \cong 1$ ), and the dynamic moduli increase more gently. This can be correlated with a small increase of the PNIPA concentration inside the microdomains, with or without some reorganization at the mesoscopic level. For the PD-N sample, this strong segregation regime where all PNIPA side-chains are embedded into aggregates, is observed only at higher temperature; typically above 55 °C. In these conditions where most PNIPA side-chains participate to the association behavior the invariant analysis shows that the microdomains are not totally dry and contain around 20 to 30 wt% of water. This result is in good agreement with the literature that generally describes the phase transition of PNIPA by the formation of glassy-like aggregates; the glass transition of the PNIPA/water system being close to room temperature for PNIPA volume fraction around 70 wt% [21].

From the asymptotic behavior obtained at high temperature ( $I(q) \sim q^{-4}$ ), the total interface area of microdomains ( $S$ ) in the

scattering volume ( $V$ ) can be calculated using the following relation:

$$S_{\text{spe}} \cong \frac{S}{V\phi_2\phi_1} = \frac{\pi}{Q} \lim_{q \rightarrow \infty} q^4 I(q) \quad (3)$$

As  $V\phi_2$  is the total volume of microdomains and  $\phi_1$  is close to 1 for all the copolymer solutions in the segregated regime, the left hand term in equation (3) can be identified with the specific surface of PNIPA microdomains ( $S_{\text{spe}}$ ). Interestingly, at high temperature, this specific surface is almost the same whatever the topology (PN-D or PD-N) and the concentration of copolymers ( $C_p = 3$  and 8 wt%):  $S_{\text{spe}} 0.022 \text{ \AA}^{-1}$ . One could see perhaps some close relation with the internal structure of the *Yin and Yang* copolymers having similar PDMA/PNIPA composition (close to 50/50). While the specific surface can be easily calculated, the real size of the microphase separated domains cannot be precisely determined. Indeed domains size is closely related to the possible morphology:  $S_2/V_2$  being equal to  $1/t$  for platelets of thickness  $t$  ( $t = 46 \text{ \AA}$ ),  $2/R$  for cylinders of radius  $R$  ( $R = 93 \text{ \AA}$ ),  $3/R$  for spheres of radius  $R$  ( $R = 140 \text{ \AA}$ ) and  $4/\xi$  or  $6/\xi$  for various random biphasic models with a correlation distance  $\xi$  ( $\xi = 186$  or  $280 \text{ \AA}$ , respectively) [46–48].

### 3.5. Concentration dependence

As shown in supporting information (Fig. S5), there is no major difference concerning the thermodynamic behavior as a function of the copolymer concentration. Indeed, for both series of copolymer solutions, the same endotherm with similar association temperature and enthalpy were obtained whatever is the concentration investigated between 1 and 10 wt%. Looking at the macroscopic properties, the conclusion is rather different. For simplicity we have plotted in Fig. 9 the complex viscosity versus the temperature as this single parameter  $\eta^*$  is proportional to both loss and storage moduli in the liquid (solution) and solid (gel) states, respectively. Working at low concentration (1 wt%), in the semi-dilute regime, the PD-N solution exhibits a very weak increase of viscosity above 40 °C (about 1 decade) followed by thermo-thinning at higher temperatures. In this case, the elastic modulus remains negligible at all temperatures and the solution is mainly viscous. While 1 wt% is too low to form a percolating network with the PD-N copolymer, this situation becomes more favorable at higher concentrations as a dramatic increase of elasticity and complex viscosity is observed from 2 wt%. In the case of the PN-D sample, the formation of an elastic network at high temperature is obtained at higher concentration than PD-N, typically 3 wt%. Indeed, the solution at 1 wt%

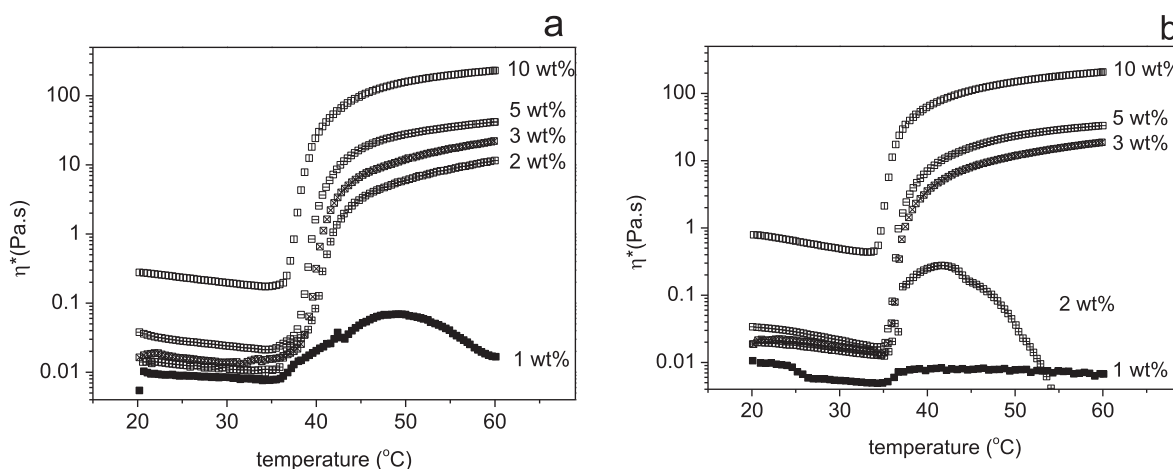
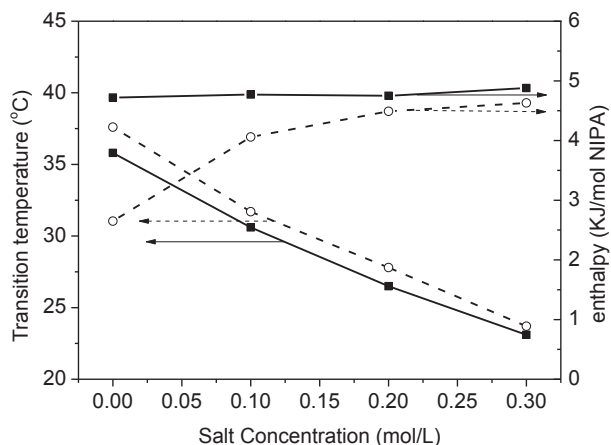


Fig. 9. Temperature dependence of viscoelastic properties of PD-N (a) and PN-D (b) aqueous solutions as a function of polymer concentration ( $f = 1 \text{ Hz}$ , heating rate =  $2 \text{ °C min}^{-1}$ ).



**Fig. 10.** Influence of added potassium carbonate on the association behavior of 3 wt% aqueous solutions of PD-N (○ and dash line) and PN-D (■ and solid line). (heating rate = 2 °C min<sup>-1</sup>).

does not really show any thermoviscosifying effect while, at 2 wt%, only a weak thermothickening is observed between 35 and 40 °C followed by a collapse of the macromolecular assembly at higher temperature.

Even if both the level of viscosity and concurrently the level of overlapping of copolymers PD-N and PN-D are similar at low temperature and the average molar mass of PN-D is higher than PD-N, we have to consider that contrary to PD-N, the PN-D sample undergoes a strong collapse of its pervaded volume at the transition threshold. There is consequently an important competition between intra- and inter-chain associations in the vicinity of the transition temperature and concentration will have a huge impact on the connectivity of the self-assembly. Conversely, as the PDMA backbone has a weak temperature dependence, we can reasonably assume that inter-chain associations will become favorable as soon as the overlapping of the chains will be effective in the low temperature range. Whatever is the copolymer, stable and thermoreversible gels are readily obtained above the critical percolation concentration.

### 3.6. Addition of salt

It is well known that the addition of salts in aqueous media generally destabilizes the hydration state of LCST polymers and

leads to a decrease of their transition temperature. This effect, known as salting-out, has been extensively used to control the phase separation on a very broad range of temperature [17] that can extend well beyond  $\Delta T = 100$  °C. In the present study we have used potassium carbonate which is known to strongly modify the solubility of PNIPA. As shown in Fig. 10, the addition of K<sub>2</sub>CO<sub>3</sub> 0.3 M decreases the association temperature from 36–38 °C to 23 °C in a very similar manner for the two copolymers.

We can also notice that the addition of salt increases the transition enthalpy of the PD-N sample that reaches about 4.5–4.7 kJ/mol of NIPA like the PN-D copolymer and the graft PNIPA precursor as well. We can assume that the dehydration process of PNIPA grafts with formation of intra-molecular hydrogen bonding is more efficient at high temperature in the presence of salt.

The viscoelastic properties of the same solutions, reported in Fig. 11, display a dramatic difference between the two copolymers. In the case of PD-N, with PNIPA grafts, the addition of salt mostly shifts the association temperature along the x-axis towards lower temperature as observed from DSC. The complex viscosity or dynamic moduli only show a weak decrease with added salt that can be related to a slight deswelling of the PDMA backbone as the quality of solvent becomes worse. This behavior is well documented with solutions of poly(sodium acrylate) grafted with poly(ethylene oxide) which have been studied on a very high range of K<sub>2</sub>CO<sub>3</sub> concentrations (up to 1.2 M) [49]. By comparison, the impact of salt on a 3 wt% PN-D solution is much more critical as the percolation and thermothickening properties rapidly vanish. Indeed, if addition of salt effectively decreases the association temperature, only a weak thermothickening is observed with K<sub>2</sub>CO<sub>3</sub> 0.1 M with a decrease of the moduli at high temperature of more than one decade compared to the same solution in pure water. Beyond these conditions, the formation of non percolating clusters in the solution gives rise to an unstable viscous behavior. Similarly, neutron scattering data show a better stability of the micro-phase separated PD-N sample in the presence of salt, compared to PN-D (see Fig. S6 in Supporting Information). These experiments, probing the structure at a local scale, point out a large increase of the characteristic length of microphase separation (more than 50%) when K<sub>2</sub>CO<sub>3</sub> 0.3 M is added into the PN-D solution while this characteristic size remains almost unchanged with the PD-N sample. In this later case the main difference arises from the formation of a more concentrated PNIPA phase at high temperature as already underlined by DSC thermograms. Even if there is a lack of information at the mesoscopic scale, that could bridge neutron scattering to rheology, we can assume that the high sensitivity of

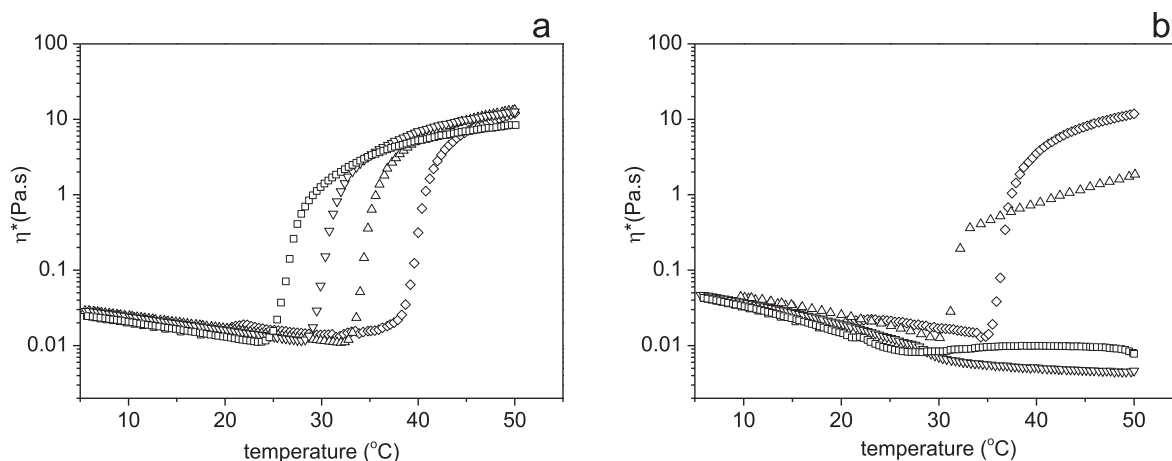


**Fig. 11.** Influence of salt on viscoelastic properties of PD-N (a) and PN-D (b) aqueous solutions ( $C_p = 3$  wt%,  $f = 1$  Hz, heating rate = 2 °C min<sup>-1</sup>). K<sub>2</sub>CO<sub>3</sub> concentrations: 0 (◇), 0.1 (△), 0.2 (▽) and 0.3 mol/L (□).

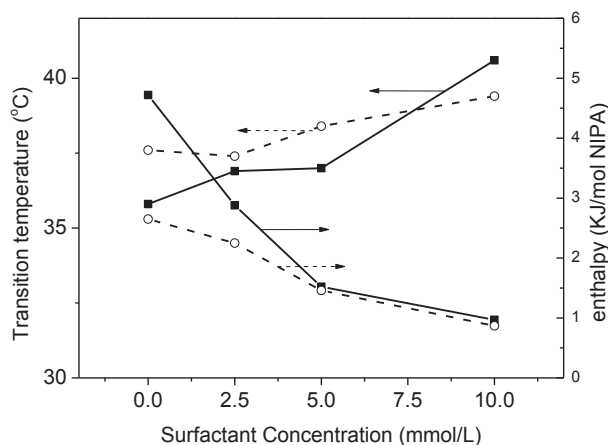


**Fig. 12.** Influence of added SDS on the association behavior of 3 wt% aqueous solutions of PD-N (○ and dash line) and PN-D (■ and solid line). (heating rate = 2 °C min<sup>-1</sup>).

the PNIPA backbone in the vicinity of the phase transition and its lower stability in the presence of salt are responsible for the weak thermothickening performance observed at 3 wt%. This problem can nevertheless be avoided by working at higher polymer concentration where inter-chain association will dominate over the intra-molecular collapse occurring during the micro-phase separation (see Fig. S7 in Supporting Information).

### 3.7. Addition of surfactant

The addition of ionic surfactant, either anionic such as SDS (sodium dodecyl sulfate) or cationic like CTAC (cetyltrimethyl ammonium chloride), is known to dramatically modify the phase transition of PNIPA derivatives in aqueous solution. In the case of SDS, it was proposed that above a critical aggregation concentration (~0.8 mM), that is well below the critical micelle concentration of SDS (8.6 mM), surfactant micelles bound to PNIPA segments via hydrophobic interactions, forming polyelectrolyte necklaces that progressively hinder the formation of PNIPA aggregates at high temperatures [41,50,51]. Indeed, as shown in Fig. 12, the addition of SDS into PD-N and PN-D solutions has the opposite effect of salt with an increase of the association temperature and a decrease of the transition enthalpy. A weaker segregation state at high temperature was also observed by <sup>1</sup>H NMR in the presence of 2.5 mM of

SDS (Fig. S8 in Supporting Information). We can also mention that from 2D NOESY experiments (not shown here) it was emphasized that in the range of concentration studied, SDS molecules efficiently interact with NIPA units, as already reported in the literature [30], but not with DMA. Again the two copolymers behave very similarly from the thermodynamic point of view but their macroscopic properties are totally different at this polymer concentration.

As shown in Fig. 13, the viscoelastic properties of the PD-N solution is shifted to higher temperature with increasing SDS concentration in agreement with DSC data. Concurrently the thermothickening properties progressively decrease and we could expect to totally suppress the thermoassociation behavior at very high SDS concentrations, when all PNIPA chains will be saturated by surfactant micelles forming water-soluble polyelectrolyte necklaces [50]. Such behavior is expected at high temperature for weight ratio SDS/PNIPA (S/P) higher than 0.4 [41,50], i.e. SDS concentration higher than 20 mM in our conditions. By comparison, the sol/gel transition is totally suppressed for the PN-D solutions, even for the lowest concentration of added surfactant (2.5 mM, i.e. S/P ≈ 0.05). In this case, where the gelation threshold relies on the percolation of PNIPA aggregates, the solubilization of PNIPA chains or sequences with the formation of polyelectrolyte necklaces will be critical for the percolation process, especially at 3 wt% which is just above the concentration threshold. The neutron scattering data plotted in supporting information (see Fig. S6) also indicate a higher sensitivity of the PN-D sample with added SDS as the characteristic length is reduced from about 15%,  $q_{max}$  being shifted towards higher  $q$  values. For the two samples, the relative concentration  $f_{PNIPA} \cdot \phi_{PNIPA}$  that can be calculated from the invariant highlights a decrease of 10–20% when 2.5 mM SDS is added, in very good agreement with DSC and NMR experiments (see Fig. S8 in Supporting Information). As directly shown by NMR, this result can be attributed to the decrease of the number of PNIPA sequences that participate to the association process ( $f_{PNIPA} < 1$ ).

### 3.8. Self-assembling in dilute solution

Dynamic Light Scattering (DLS) has been used to investigate the variation of the size distribution profile of copolymer chains during the phase transition process. For that purpose very dilute solutions (0.01 wt%) have been prepared at room temperature and the size of the copolymer chains was followed as a function of temperature. The results reported in Table 2 show that the PN-D chain with the PNIPA backbone has a high tendency to collapse upon heating. Its

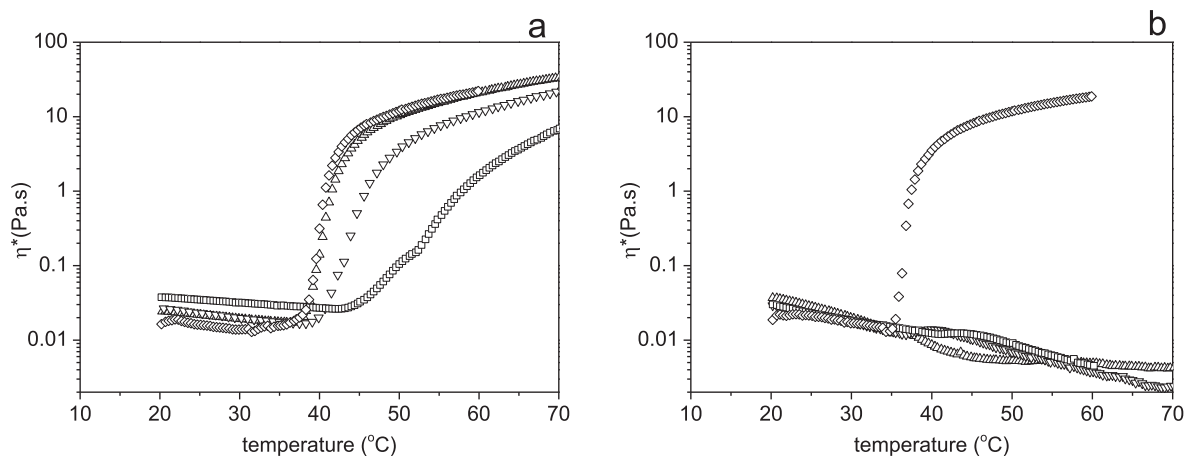


**Fig. 13.** Influence of SDS on viscoelastic properties of PD-N (a) and PN-D (b) aqueous solutions ( $C_p = 3$  wt%,  $f = 1$  Hz, heating rate = 2 °C min<sup>-1</sup>). SDS concentrations: 0 (◇), 2 (△), 5 (▽) and 10 mM (□).

**Table 2**  
Dynamic light scattering of copolymers in dilute solutions.

Solvent	T (°C)	Radius (nm)		PDI	
		PN-D	PD-N	PN-D	PD-N
H <sub>2</sub> O <sup>a</sup>	25	37	33	0.25	0.25
H <sub>2</sub> O <sup>a</sup>	35	29	25	0.29	0.26
H <sub>2</sub> O <sup>a</sup>	45	17	47	0.06	0.24
H <sub>2</sub> O <sup>a</sup>	55	14	36	0.04	0.25
H <sub>2</sub> O <sup>b</sup>	55	34	—	0.27	—
[K <sub>2</sub> CO <sub>3</sub> ] 0.1 M <sup>a</sup>	55	76	60	0.39	0.43
[SDS] 2.5 mM <sup>a</sup>	55	24	18	0.32	0.37

<sup>a</sup> Samples were prepared at concentration 0.1 g/L at room temperature and used for test at designate temperature directly.

<sup>b</sup> Samples were initially prepared at 30 g/L at room temperature and left at 55 °C for 1 h. Then the sample was diluted by water (55 °C) and used for test at 55 °C.

pervaded volume decreases 20 times between 25 and 55 °C but the collapsed conformation remains stable with a steric corona formed by PDMA side-chains.

This result is in good agreement with the theoretical predictions of Borisov and coworkers concerning the conformation of comb-like copolymers upon inferior solvent strength for the main chain while the solvent remains good for the side chains [30,31]. Indeed, in the case of weakly asymmetric graft copolymers, as it is for the PN-D sample where the size of the individual side chain in good solvent is close to the average size of the spacer under  $\Theta$ -conditions, they predict the formation of stable collapsed structures (necklace of star-like micelles) in poor solvent conditions for the backbone. The main difference between our copolymers and the theoretical predictions is that dynamics is highly reduced in the case of PNIPA assemblies.

If the phase transition is activated in the semi-dilute regime (3 wt%) prior to dilution, aggregates of higher polydispersity are obtained, showing their propensity to form inter-molecular aggregates at higher concentration. By comparison, PD-N chains studied in dilute conditions show larger dimensions above the transition temperature with the formation of both intra- and inter-molecular associations. This behavior is very similar to the self-assembly of polysoaps reported by Borisov et al. [32] in dilute solutions where bridging attractions are responsible for inter-chain aggregation and macrophase separation. Although addition of salt

favors the formation of larger inter-chain aggregates, the opposite tendency is observed in the presence of SDS at high temperature.

#### 4. Discussion

As shown in this work, the solution properties of the two copolymers PD-N and PN-D, having similar compositions but inverse topologies, display close resemblance and critical differences in aqueous media.

Water-soluble copolymers grafted with LCST stickers have been well studied during the last two decades and their structure determined from scattering techniques is generally described with the formation of LCST microdomains connected by water-soluble macromolecular backbones. The exact structure strongly depends on the nature and number of the LCST stickers, but also on the nature of the backbone which could be polyelectrolyte or neutral, in very good solvent or in theta-solvent. All these parameters will have critical impacts on the microphase separation as they will control the size and the stability of domains. In the case of PDMA which could be considered in good solvent in water, the neutron scattering data obtained with PD-N solutions show a rather continuous process for the microphase separation with the formation of an increasing number of PNIPA aggregates of increasing concentration that finally leads to sharp interfaces with the outer medium at high temperature. As PNIPA chains are relatively short and chemically anchored on the hydrophilic backbone, they are less prompt to self-associate. The self-assembling is then a relatively continuous process taking place mainly between 40 and 55 °C as shown by DSC, NMR and SANS. In the schematic description of the self-assembling of PD-N sample given in Fig. 14, the main idea is that the phase transition of PNIPA side-chains (from coil to globule) leads to a micro-phase separated structure where the rich PNIPA aggregates, drawn as spheres for simplicity, can be either randomly dispersed within the PDMA/solvent matrix or connected forming a bicontinuous morphology.

In the first case, the percolation and the viscoelastic properties originate from the PDMA backbones making bridges between PNIPA domains. In the other situation, both PDMA chains and percolating PNIPA aggregates will behave as physical bridges in the macroscopic properties. By comparison, DSC, NMR and SANS data show that PN-D chains undergo an abrupt micro-phase separation above the

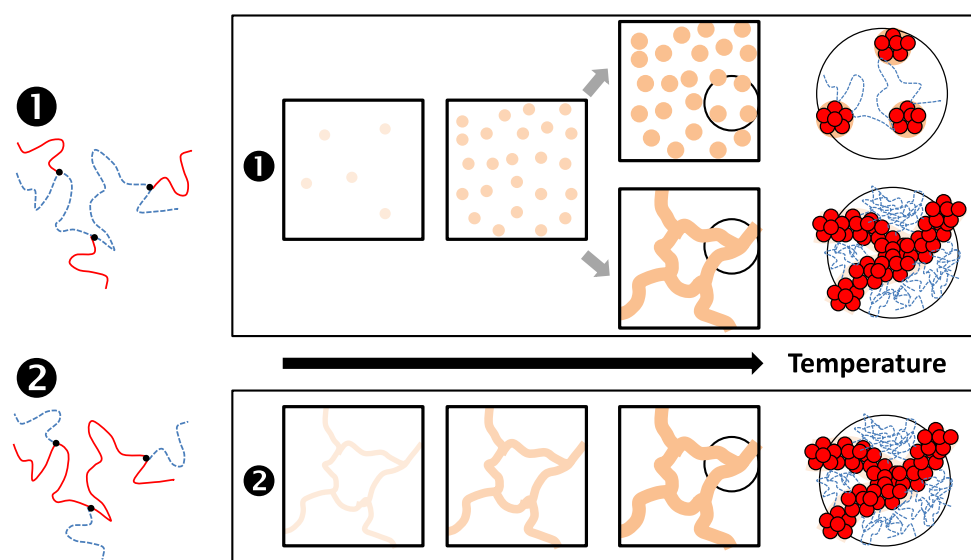


**Fig. 14.** Schematic representation of the thermoassociation behavior of PD-N (●) and PN-D (●) copolymers in aqueous media.

transition temperature that rapidly leads to the formation of concentrated PNIPA domains with sharp interface. Contrary to the copolymer with PNIPA side-chains, the phase transition of the PNIPA backbone is almost achieved between 35 and 40 °C. Above this temperature, the mobility of PNIPA, as seen by NMR, is highly reduced in agreement with the vicinity of the glass transition of the binary PNIPA/water system, and the slight increase of composition observed at higher temperatures can be attributed to a continuous release of water from the aggregates. As PN-D chains are able to form a stable percolating network with elastic properties above 3 wt %, we can reasonably assume that PNIPA sequences of the backbone self-assemble into a bicontinuous two-phase structure. According to the schematic description given in Fig. 14, PNIPA sequences inserted between PDMA side-chains collapse above their transition temperature and form sticky globules that self-associate into a percolating 3D structure. This mechanism can be compared to the one reported with aqueous solutions of pure linear PNIPA as they also form physical networks during phase separation above some overlap concentration [52,53]. Nevertheless for pure PNIPA, the non-equilibrium morphologies, which are kinetically controlled, are much less stable with time or under high deformation. This is not the case with graft copolymers, PD-N and PN-D, as PDMA sequences stabilize in water the morphologies above the LCST and the macroscopic properties remain totally reversible by cycling the temperature. The fact that we also consider in Fig. 14 the possibility for PD-N chains to form a percolating network of PNIPA aggregates, like PN-D, comes from the strong similarity of their viscoelastic properties in spite of their inverse topologies. On the one hand, this similarity is quite reasonable for the complex viscosity at low temperature as, in the non-associating state, similar solubility and swelling behaviors are expected for the two copolymers having close average molar masses and composition. As shown in Fig. 15, the viscosities are in agreement with theoretical scaling exponents calculated for unentangled ( $x = 5/4$ ) and entangled ( $x = 15/4$ ) semi-dilute solutions of polymer in good solvent [54]; the entangled regime starting around 5 wt%. Quantitatively, the overlap concentration can be calculated at 25 °C from the radius of gyration ( $R_G = 35$  nm in Table 2) and the molar mass of the copolymers ( $M = 400\,000$  g/mol; see Table 1). This gives  $C^* \approx 0.4$  wt% for both PN-D and PD-N, in good agreement with experimental data of Fig. 9 if we assume that the solution viscosity at  $C^*$  should be twice the viscosity of the solvent ( $\eta \approx 0.002$  Pa.s) [55]. Similarly, if we consider that  $C^*$  is about 0.4 wt% for both copolymer samples, this means that at 5 wt% each chain overlaps with at least 10 others which is a good criterion for the beginning of the entangled regime according to Dobrynin et al. [56].

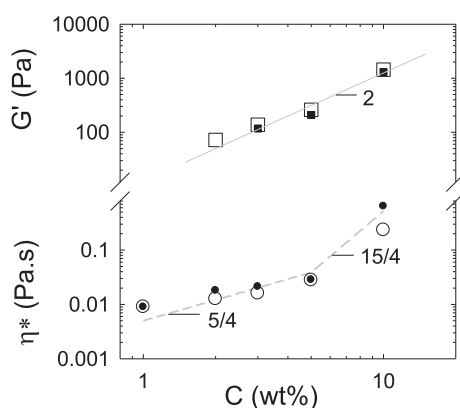


Fig. 15. Concentration dependence of complex viscosity at 20 °C (○●) and elastic modulus at 60 °C (□■) for PD-N (hollow symbols) and PN-D (filled symbols) aqueous solutions. Dotted lines are used as guide lines.

While these rheological data are quite expected at room temperature, the results are more surprising at high temperature where similar elastic moduli were obtained for both PN-D and PD-N solutions. This leads us to believe that a similar self-assembly of PN-D and PD-N in water underlies their macroscopic properties.

In this framework, one of the main features of the micro-phase separation of PNIPA sequences is the important slowing down of the polymer dynamics. The “glassy” behavior, or more precisely the low dynamics of PNIPA aggregates, is of prime importance as the lifetime of the associations is responsible for the covalent-like 3D network observed at high temperature. Moreover the abrupt transition of the PN-D sample, together with the formation of concentrated aggregates of low mobility, gives the possibility to freeze the micro-phase separated structure during the early stage of the transition.

In the case of PN-D solution, the concentration is a critical parameter and a stable thermo-thickening behavior was observed only at a sufficiently high concentrations (3 wt% and above), mainly in the semi-dilute entangled regime where intermolecular associations overcome the intramolecular collapse of the chains. Below this concentration, the formation of loosely connected or unconnected clusters will only provide poor viscous properties. On the other hand, the PD-N copolymer is more stable at lower concentration (below 3 wt%): this gives rise to viscosity enhancement through the formation of PDMA bridges between unconnected PNIPA clusters.

It is interesting to notice that when stable gels are formed, either with PN-D or PD-N, they exhibit very similar elastic modulus at the same polymer (or PNIPA) concentration with a quadratic dependence of  $G'$  on concentration (see Fig. 15).

Taking into account the picture of a bicontinuous structure, where the mechanical properties are mainly brought by the concentrated PNIPA phase, this mechanical behavior is comparable with open-cell polymer foams where the elastic modulus of the material varies with the modulus of the wall and the square of their volume fraction [57]. Working close to the concentration threshold of the copolymers (3 wt%), the addition of salt or surfactant reveals real differences with opposite macroscopic behaviors. For the PD-N sample, addition of salt (or SDS) decreases (or increases) the association temperature as expected from the solubility of PNIPA chains. These additives also modify the elastic modulus in the gel state as 1) salt slightly deswells the PDMA backbone, decreasing the degree of overlapping, and 2) SDS decreases the number of PNIPA stickers by forming polyelectrolyte necklaces. On the other hand, while the shift of the association temperature is similar for PN-D compared to PD-N, both salt and SDS dramatically ruins the 3D scaffold initially formed in water. In the first situation, the loss of connectivity can be correlated to a lower stabilization of PNIPA domains by PDMA hydrophilic side-chains; the characteristic wavelength of the microphase separation increasing with salt concentration. In the presence of SDS, the opposite effect is observed with the formation of smaller PNIPA aggregates which become more repulsive with the binding of SDS molecules.

## Acknowledgments

We gratefully acknowledge the financial support of CNRS, ESPCI and UPMC, the China Scholarship Council for the PhD fellowship funding of Hui Guo and CEFIPRA for promoting Indo-French collaboration. The authors also thank Dr Guylaine Ducouret for technical advice on performing rheological measurements.

## Appendix A. Supplementary data

Supplementary data related to this article can be found at <http://dx.doi.org/10.1016/j.polymer.2015.01.038>.

## References

- [1] Polymers in aqueous media: performance through association. In: Edward Glass J, editor. *advances in chemistry series*; 1989. p. 223.
- [2] Taylor KC, Nasr-El-Din HA. *J Petrol Sci Eng* 1998;19:265–80.
- [3] Wever DAZ, Picchioni F, Broekhuis AA. *Prog Polym Sci* 2011;36:1558–628.
- [4] Dimitrov I, Trzebicka B, Müller AHE, Dworak A, Tsvetanov CB. *Prog Polym Sci* 2007;32:1275–343.
- [5] Schattling P, Jochum FD, Theato P. *Polym Chem* 2014;5:25–36.
- [6] Barabanova A, Molchanov V, Philippova O, Khokhlov A. *Macromol Symp* 2014;337:80–6.
- [7] Liu R, Fraylich M, Saunders BR. *Colloid Polym Sci* 2009;287:627–43.
- [8] L'Alloret F. U.S. Patent US7115255, 2001.
- [9] Maroy P, Hourdet D, L'Alloret F, Audebert R. *European Patent EP0583814*, 1993.
- [10] Drury JL, Mooney DJ. *Biomaterials* 2003;24:4337–51.
- [11] Gutowska A, Jeong B, Jasionowski M. *Anat Rec* 2001;263:342–9.
- [12] Bhattarai N, Ramay HR, Gunn J, Matsen FA, Zhang M. *J Control Release* 2005;103:609–24.
- [13] Cohn D, Sosnik A, Garty S. *Biomacromolecules* 2005;6:1168–75.
- [14] Heymann E. *Trans Faraday Soc* 1935;31:846–64.
- [15] Klug ED. *J Polym Sci Part C* 1971;36:491–508.
- [16] Durand A, Hervé M, Hourdet D. Stimuli-responsive water soluble and amphiphilic polymers. In: McCormick CL, editor. *ACS Symposium series 780*. Washington, DC: American Chemical Society; 2000. p. 181–207. Chapter 11.
- [17] Hourdet D, L'Alloret F, Audebert R. *Polymer* 1994;35:2624–30.
- [18] Hourdet D, L'Alloret F, Durand A, Lafuma F, Audebert R, Cotton J-P. *Macromolecules* 1998;31:5323–35.
- [19] Bromberg L. *Macromolecules* 1998;31:6148–56.
- [20] Durand A, Hourdet D. *Polymer* 1999;40:4941–51.
- [21] Petit L, Karakasyan C, Pantoustier N, Hourdet D. *Polymer* 2007;48:7098–112.
- [22] Karakasyan C, Lack S, Brunel F, Maingault P, Hourdet D. *Biomacromolecules* 2008;9:2419–29.
- [23] Siband E, Tran Y, Hourdet D. *Macromolecules* 2011;44:8185–94.
- [24] Afroz F, Nies E, Berghmans HJ. *Mol Struct* 2000;554:55–68.
- [25] Aseyev V, Tenhu H, Winnik FM. *Adv Polym Sci* 2010;242:29–89.
- [26] Philipp M, Müller U, Aleksandrova R, Sanctuary R, Müller-Buschbaum P, Krüger JK. *Soft Matter* 2012;8:11387–95.
- [27] Balu C, Delsanti M, Guenoun P. *Langmuir* 2007;23:2404–7.
- [28] László K, Guillermo A, Flueraşu A, Moussaïd A, Geissler E. *Langmuir* 2010;26:4415–20.
- [29] Braun O, Boué F, Candau F. *Eur Phys J* 2002;E7:141–51.
- [30] Borisov OV, Zhulina EB. *Macromolecules* 2005;38:2506–14.
- [31] Kosovan P, Kuldova J, Limpouchova Z, Prochazka K, Zhulina EB, Borisov OV. *Macromolecules* 2009;42:6748–60.
- [32] Borisov OV, Halperin A. *Curr Opin Colloid Interface Sci* 1998;3:415–21.
- [33] Gottlieb HE, Kotlyar V, Nudelman A. *J Org Chem* 1997;62:7512–5.
- [34] Hourdet D, Gadgil J, Podhajecka K, Badiger MV, Brûlet A, Wadgaonkar PP. *Macromolecules* 2005;38:8512–21.
- [35] Hourdet D, Petit L. *Macromol Symp* 2010;291–292:144–58.
- [36] Schild HG, Tirell DA. *J Phys Chem* 1990;94:4352–6.
- [37] Otake K, Inomata H, Konno M, Saito S. *Macromolecules* 1990;23:283–9.
- [38] Patel T, Ghosh G, Yusa S-I, Bahadur PJ. *Dispers Sci Technol* 2011;32:1111–8.
- [39] Badiger MV, Rajamohanam PR, Kulkarni MG, Ganapathy S, Mashelkar RA. *Macromolecules* 1991;24:106–11.
- [40] Lele AK, Hirve MM, Badiger MV, Mashelkar RA. *Macromolecules* 1997;30:157–9.
- [41] Durand A, Hourdet D, Lafuma F. *J Phys Chem B* 2000;104:9371–7.
- [42] Rusu M, Wohlrab S, Kuckling D, Möhwalld H, Schönhoff M. *Macromolecules* 2006;39:7358–63.
- [43] Shibayama M, Tanaka T, Han CC. *J Chem Phys* 1992;97:6829–41.
- [44] Petit L, Bouteiller L, Brûlet A, Lafuma F, Hourdet D. *Langmuir* 2007;23:147–58.
- [45] Shibayama M, Tanaka T, Han CC. *J Chem Phys* 1992;97:6842–54.
- [46] Auvray L, Cotton J-P, Ober R, Taupin C. *J Phys* 1984;45:913–28.
- [47] Barnes IS, Hyde ST, Ninham BW, Derian P-J, Drifford M, Zemb T. *J Phys Chem* 1988;92:2286–93.
- [48] Teubner M, Strey RJ. *Chem Phys* 1987;87:3195–200.
- [49] L'Alloret F, Hourdet D, Audebert R. *Colloid Polym Sci* 1995;273:1163–73.
- [50] Lee L-T, Cabane B. *Macromolecules* 1997;30:6559–66.
- [51] Chen J, Xue H, Yao Y, Yang H, Li A, Xu M, et al. *Macromolecules* 2012;45:5524–9.
- [52] Yang Y, Zeng F, Tong Z, Liu X, Wu S. *J Polym Sci Part B Polym Phys* 2001;39:901–7.
- [53] Kressler J, Kammer H-W. In: Binder WH, editor. *Self-healing polymers: from principles to applications*. Weinheim: Wiley-VCH Verlag GmbH; 2013. p. 139–52. Chapter 5.
- [54] Rubinstein M, Semnov AN. *Macromolecules* 1998;31:1386–97.
- [55] Colby RH. *Rheol Acta* 2010;49:425–42.
- [56] Dobrynin AV, Colby RH, Rubinstein M. *Macromolecules* 1996;28:1859–71.
- [57] Ashby MF. *Metall Mater Trans A* 1983;14:1755–69.